Rydberg Fingerprint Spectroscopy: A New Spectroscopic Tool with Local and Global Structural Sensitivity

Jaimie L. Gosselin and Peter M. Weber*

Department of Chemistry, Brown University, Providence, Rhode Island 02912

Received: January 21, 2005; In Final Form: March 27, 2005

Rydberg spectra are shown to provide a spectral fingerprint that is sensitive to molecular structure in unique ways. The concepts are demonstrated using a set of isomeric fluorophenols and a sequence of aliphatic diamines. In the fluorophenols, the sensitivity extends to the placement of a single hydrogen atom and can be traced to the molecular charge distributions associated with the locations of atoms and functional groups with respect to the charge center. Experiments on tetramethyl diamines demonstrate that the structural sensitivity encompasses the extended molecular structure, including parts of the molecule that are remote from the ionization center. This global structure sensitivity makes Rydberg fingerprint spectroscopy uniquely suited to characterize structures of large-scale molecular systems.

The determination and characterization of molecular structures are of great importance to chemistry. Although the determination of structures is most important for developing a fundamental understanding, chemistry is often better served with sensitive methods merely to characterize molecular structures. In that context, mass spectrometry has acquired an important standing because it combines the ability to distinguish between different molecules with an astonishing sensitivity and almost universal applicability. Nevertheless, mass spectrometry alone is often insufficient to identify molecular compounds because the measurement of the mass is not sufficiently deterministic to positively identify anything but the smallest molecular structures. As a result, mass spectrometry is often coupled with other analytical techniques, such as chromatography or a second stage of mass spectrometry. Such secondary techniques must exhibit a chemical or structural sensitivity that adds at least one dimension to the otherwise one-dimensional mass spectrum. Moreover, it must be possible to couple the secondary technique to the mass spectrometer without unduly increasing the complexity of the instrument.

In this article, we show that Rydberg spectroscopy meets those demands. Rydberg spectra can be understood as fingerprints that are sensitive to molecular structures in unique ways, providing them with sensitivity from minute structural aspects to global structural features. These characteristics, together with the possibility to couple Rydberg fingerprint spectroscopy with mass spectrometry, make the method an attractive choice for many analytical applications involving large molecular systems.

Molecular Rydberg states derive from the electronic states of the hydrogen atom. In hydrogen, the binding energy of the electron (i.e., the energy difference between the electron at rest at an infinite distance and the bound electron) is dependent only on the principal quantum number n

$$E_B = \frac{Ry}{n^2}$$

where Ry is the Rydberg constant (13.606 eV). In atoms larger than hydrogen and in molecules, the loss of symmetry makes the binding energy dependent on the angular momentum state of the Rydberg orbit. To a good approximation, the binding energy of a Rydberg electron in a molecule is given by

$$E_B = \frac{Ry}{(n-\delta)^2}$$

where δ, called the quantum defect, is approximately constant for a given orbital angular momentum.[1,2] Typical quantum defects range from 0 to 1. Orbitals with small angular momentum have wave functions that penetrate into the inner parts of the Coulomb potential and are therefore sensitive to the local distribution of charges, atoms, and functional groups. Thus, typical values of quantum defects are close to 1 for s orbitals, 0.3−0.5 for p orbitals, and ≤0.1 for d and higher angular momentum states.[3]

In a recent publication, Kuthirummal and Weber have shown that the spectrum of binding energies of Rydberg orbitals, which can be analyzed and assigned in terms of their principal quantum numbers and quantum defects, is sensitive to the molecular shape and can therefore be interpreted as a structure-sensitive spectral fingerprint.[4] Figure 1 illustrates the origin of the structure sensitivity of Rydberg levels. The Coulomb interaction between a proton and the electron (dashed line) is in molecules modified at small distances by the combination of repulsive and attractive charges of all of the component charges of the molecule. The electrostatic potential at small distances is therefore determined by the placement of atoms, functional groups, and partial charges. Although the wave function of the molecular Rydberg state at large distance mimics that of the hydrogen atom, it incurs additional phase shifts near the ion core. Because the wave function has to constructively interfere with itself upon completing a round trip, those phase shifts lead to an adjustment of the energy from the value in the hydrogen atom, E_{Rn}, to a new value E'_{Rn}. Because the phase shift is sensitive to the placement of the charges, it can be understood that the Rydberg-level energies encode the molecular structure.

To be useful as an analytical tool, an efficient method to acquire Rydberg spectra is needed. The present work employs

* Corresponding author. E-mail: peter_weber@brown.edu. Fax: +1-401-863-2594.

10.1021/jp0503866 CCC: $30.25
Published on Web 05/14/2005

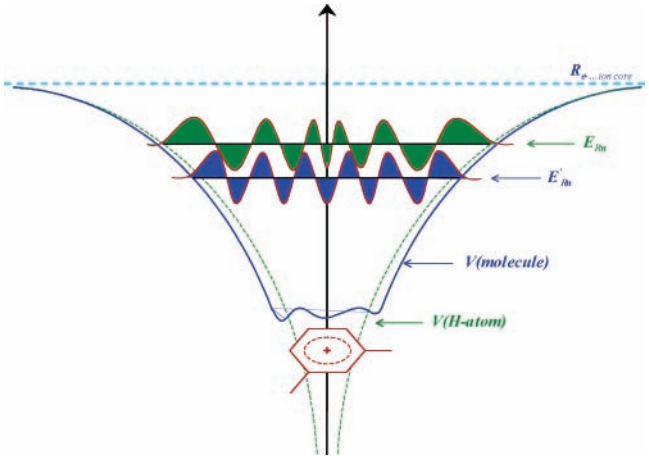

Figure 1. Wave function of a molecular Rydberg state experiences phase shifts relative to that of the hydrogen atom on account of its passage through the ion core, where the electrostatic potential, $V(molecule)$, is characteristic of the molecular structure. As a result, the energies of molecular Rydberg states, E'_{Rn}, are shifted from those of the hydrogen atom, E_{Rn}.

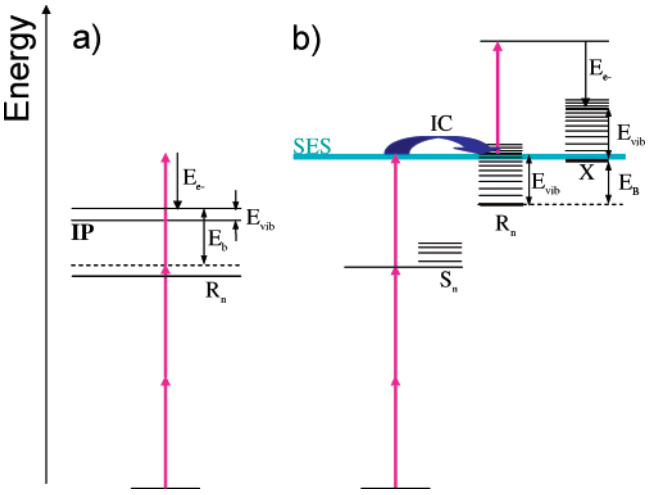

Figure 2. (a) Two-photon excitation of a Rydberg level, R_n, followed by ionization. (b) Three-photon excitation to a Rydberg level via an excited valence state, S_n, and a superexcited state, SES. In either case, the binding energy E_B, which is the difference between the ground-state energy of the ion, X, and the energy of the Rydberg state, is obtained by measuring the energy E_{c-} of the outgoing electron. The vibrational energy E_{vib} remains conserved during the ionization from the Rydberg state.

two distinct ionization schemes. In the scheme of Figure 2a, the molecule is excited in a two-photon process directly to a Rydberg state. If the potential energy surface of the Rydberg state is displaced from that of the ground state, then a single laser wavelength can induce transitions to several Rydberg levels, each containing different amounts of vibrational energy. In the ionization step, which is induced by the absorption of a third photon, the vibrational energy is conserved so that the final ion state reveals the vibrational energy content and thus the Rydberg level's energy.[5,6] The second method (Figure 2b) employs a superexcited state (SES) or highly excited valence state as a stepping stone to access many Rydberg levels. Superexcited states can be reached in a multiphoton process via intermediate electronic resonances;[5] the present work employs a three-photon process. Nonradiative relaxation leads to a set of low-n Rydberg states. A fourth photon ionizes out of the Rydberg state, generating vibrationally highly excited ions in the ground electronic state. In both schemes, the kinetic energy spectrum of the outgoing electrons (i.e., the photoelectron spectrum) reveals the final ion energies and, by inference, provides a record of the energy-level structure of the intermediate Rydberg states. Detailed investigations, including time-resolved probes of the ionization spectrum, on phenol[5−7] as well as on 1,3-cyclohexadiene and its isomers[4,8] have affirmed the nature of the described photoionization pathways. We have found the ionization mechanisms to be widely applicable, with further test systems including toluene, indole, phenanthrene, azulene, and many others. This apparently general applicability makes Rydberg fingerprint spectroscopy an intriguing technique that merits further development.

As with any new technique, it is important to establish the information content as well as limitations of the Rydberg fingerprint technique. This is particularly relevant in the present case because it remains difficult to calculate a priori the energies of Rydberg levels.[1] Even so, qualitative considerations allow us to exploit the interesting characteristics of the Rydberg fingerprints. A particularly interesting problem is that of charge migration in bifunctional molecules.[9] In a recent publication Rydberg fingerprint spectroscopy was used to calculate and control the center of the photoionization in such a bifunctional molecule by comparing with the fingerprints of the monofunctional analogs.[10]

In the present work, we examine the information content of Rydberg fingerprints by investigating two sets of molecules. The first set consists of *o*-, *m*-, and *p*-fluorophenol. The data obtained illustrates the sensitivity of Rydberg fingerprints toward charge distributions within molecules, which leads to exquisite sensitivity toward the placement of even a single hydrogen atom. The second set of molecules, a series of aliphatic diamines, explores the sensitivity of Rydberg levels toward structural changes in regions of the molecule that are remote from the ionization center, pointing to the global structure sensitivity of Rydberg fingerprint spectroscopy.

Experimental Section

The experiments are performed using a molecular beam apparatus equipped with time-of-flight mass- and photoelectron spectrometers. This instrument, which has been described in detail elsewhere,[5,10,11] is interfaced with a commercial ultrashort pulsed laser system. Femtosecond pulses of 100 fs duration are generated in a Ti:sapphire oscillator laser that is tunable in the near-infrared between 780 and 840 nm. The oscillator output is amplified to 5 μJ in a regenerative amplifier operating at a 50 kHz repetition rate and upconverted to the second harmonic using a BBO crystal, providing pulse energies of 1.2 μJ.

The laser beam is focused to an intensity of 2×10^{12} W/cm^2 and intersects the molecular beam carrying the target molecules seeded in helium. The molecules are ionized in the interaction region of the vacuum chamber with the resulting electrons ejected in all directions. Those electrons that move toward a microchannel plate detector are detected, and the signal is amplified and analyzed for the drift time using ultrafast timing electronics. The energy resolution of the photoelectron spectrometer itself exceeds 10 meV, but the resolution of the presented spectra is limited by the bandwidth of the femtosecond laser pulses. The measured quantum defects are reported to two or three significant digits, based on an error propagation analysis.

To obtain a reasonable vapor pressure, the fluorinated phenols were heated to a temperature of 70−150 °C, but the diamines were used at room temperature. All compounds were purchased from Aldrich and used without further purification. Care was taken to minimize the exposure of the diamines to water.

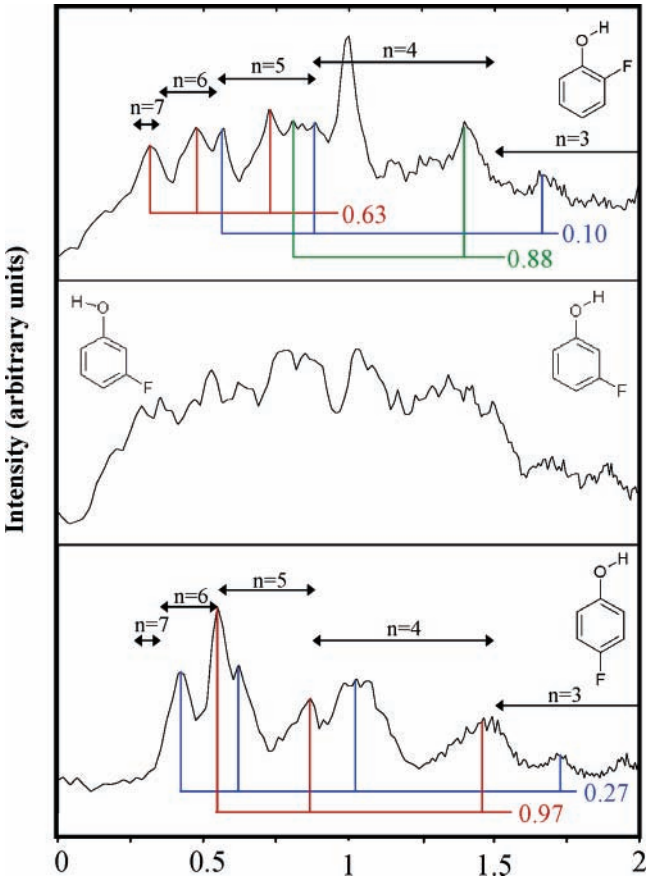

Figure 3. Rydberg fingerprint spectra of 2-fluorophenol (top), 3-fluorophenol (middle), and 4-fluorophenol (bottom) obtained with 400 nm laser pulses.

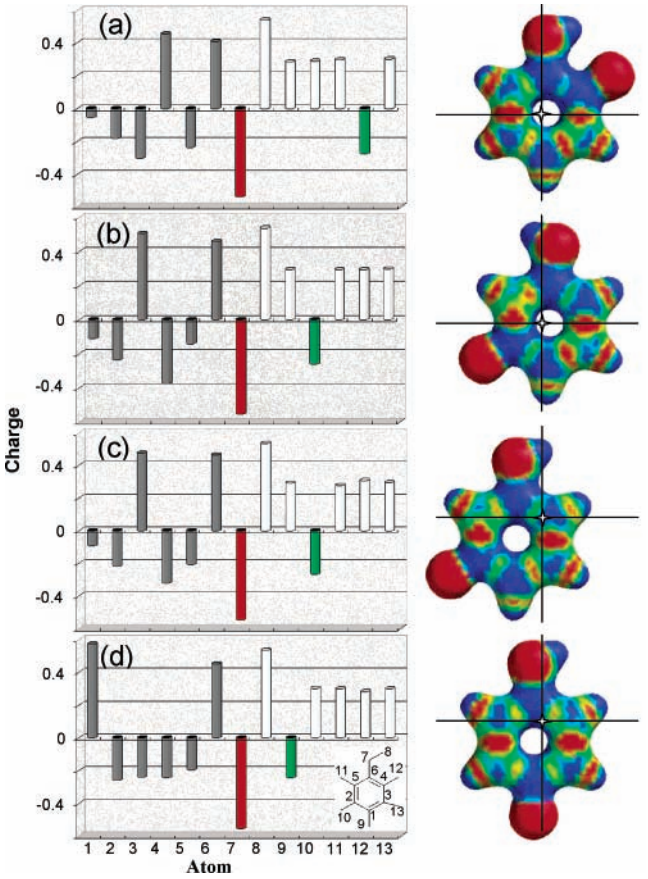

Figure 4. (Left) charge distributions in the cations of (a) 2-fluorophenol, (b and c) two conformers of 3-fluorophenol, and (d) 4-fluorophenol. The atomic positions are labeled as indicated in the inset at the bottom. The fluorine atom (green) is located at positions 12, 10, and 9, respectively. (Right) charge distributions of the respective molecular ions, with the centers of charge superimposed by crosshairs.

Results and Discussion

(i) Local Charge Distributions. The Rydberg fingerprint spectra of 2-fluorophenol (2F), 3-fluorophenol (3F), and 4-fluorophenol (4F) are shown in Figure 3. The ionization scheme employed in this set of molecules is the one illustrated in Figure 2b: Three 400 nm photons excite the molecules to superexcited states, and rapid internal conversion populates a set of Rydberg states. The fourth photon ionizes the system by ejecting the electrons.

The internal conversion step deposits a significant amount of energy into vibrational modes. Given the observed binding energies in the range of 0.5−1.5 eV and the reported ionization energies of 8.5−8.7 eV,[12] we estimate that between 1.1 and 2.3 eV of energy is deposited into vibrational modes. This large amount of vibrational energy most certainly will excite the hindered rotational motion of the hydroxy group. Nevertheless, the present experiments are not sensitive to the dynamical aspects of this motion because the laser pulse duration is shorter than the period of typical rotational motions and because the internal conversion initially deposits energy into vibrations involving the aromatic ring. For the present discussion, we therefore ignore the dynamics of the rotation of the hydrogen atom.

The Rydberg spectra of the fluorophenols exhibit a rich structure that can be assigned to Rydberg series with principal quantum numbers between 4 and 7 and several distinct quantum defect values. The most striking observations are (i) the quantum defects of 2F are quite different from those of 4F and (ii) the spectrum of 3F is too richly structured to be resolved given the spectral resolution of our instrument.

The starting point for discussing the different Rydberg fingerprint spectra of the 2F and 4F isomers is their respective structures. The molecules have atoms in different places, which gives rise to distinct phase shifts of the Rydberg wave function traversing the ion core and therefore to differences in the quantum defect values. Although this is a rational argument, it appears surprising that the differences between the isomers are as large as we observe. The carbon skeletons of the molecules are substantially the same, and the only sizable difference between the 2F and 4F isomers is the interchange of a hydrogen atom and a fluorine atom. In a first guess, one might consider phase shifts to be additive: during a round trip, the Rydberg electron might first encounter the hydrogen and then the fluorine, and on its return trip, the same atoms in reverse order. Interchanging the two atoms should therefore hardly alter the phase shifts. We conclude that additional phenomena may be at play to cause the differences between the 2F and 4F isomers.

We performed ab initio calculations for the fluorophenol cations on the B3LYP level with a 6-31G* basis set to obtain the distribution of partial charges within the molecule. Although the molecules in their Rydberg states are overall neutral, the ion cores closely resemble the molecular ions because the Rydberg electrons provide very little bonding character. The charge distributions are shown in Figure 4. It is immediately apparent that the 2F and 4F isomers have quite distinct patterns of charge distribution across the molecule. Because the Rydberg electron, on its pass through the ion core, experiences the electrostatic potential created by all of these charges, it can be seen that the overall phase shifts should be quite distinct. We

conclude that the Rydberg electron is sensitive toward the patterns of charge distribution, giving rise to the distinct Rydberg fingerprints of the 2F and 4F isomers.

The argument involving the charge distributions allows us to rationalize the different spectra of 2-fluorophenol and 4-fluorophenol. In both of those compounds, there is only a single conformer present in the molecular beam: in its ground state, the 2F molecule features a hydrogen bond between the hydroxyl hydrogen atom and the fluorine atom, which fixes the molecular structure,[13] and the 4F has only one distinct isomer based on its symmetry. The situation is more complex in 3-fluorophenol, which can have two conformeric forms present in the beam, with the hydroxyl hydrogen either in the syn or anti position with respect to the fluorine atom. Because the two forms have similar energies,[14] the Rydberg fingerprint spectrum should be a superposition of the spectra of the two forms. Even so, the distributions of charges among the atoms of the 3F molecule are almost identical in the syn and anti molecules, as seen from the bar graphs of Figure 4. Thus the question arises of why the fingerprints would be so different: how can the different placement of one hydrogen atom, while the atomic charges remain constant, cause such a dramatic effect in the Rydberg fingerprints?

To answer this question, it is useful to consider further the potential in which the Rydberg electron moves. Much of the electronic wave function of the Rydberg electron is quite far from the molecular ion core. As will be discussed in more detail below, an s or p electron in an $n = 5$ orbital has a mean diameter of about 40 Å. At this large distance, one can neglect polarization effects and express the total electrostatic potential between the electron and the molecular ion core as a multipole expansion

$$V = V_{e\text{- charge}} + V_{e\text{- dipole}} + V_{e\text{- quadrupole}} + ...$$

where the first term describes the interaction between the Rydberg electron and the positive charge of the ion core and higher-order terms derive from charge−multipole interactions.[15,16] Because the charge−multipole interactions decay rapidly with increasing distance, the dominant term at the mean Rydberg orbital radius is the interaction between the electron and the ion core. This term gives rise to the energy-level structure as expressed by the Rydberg formula. The higher-order terms, which become important as the electron passes the ion core, are then responsible for the molecule-specific quantum defects.

Using the calculated charge distributions and the molecular structures, it is possible to determine the charge centers for the fluorophenol isomers. For this calculation, we take the charge distribution as represented by the bar graphs of Figure 4 and calculate the charge centers $\mathbf{R}_c$ as

$$\mathbf{R}_c \cdot Q = \sum_i Q_i \cdot \mathbf{R}_i$$

Here, Q is the charge of the ion core (+1), and the atomic charges Q_i are at coordinates $\mathbf{R}_i$. The panels on the right side of Figure 4 show illustrations of the molecules with the positions of the charge centers marked by crosshairs. We immediately observe that the 2F and 4F isomers (top and bottom panels) have their charge centers at different positions. The distribution of partial charges about those centers is different, confirming our previous discussion. In addition, we now observe that even the charge centers of the two conformeric forms of 3F are at very different positions (two middle panels). As a result, the Coulomb potentials that determine the electron's wave function are centered at different parts of the molecule. Therefore, as seen from the Rydberg electron, the syn and anti conformers have *all* of the atoms of the molecule, and with them the distribution of charges, at very different places. Thus, even though the atomic charges are almost identical, the dependence of the charge center on the hydrogen atom position causes the entire distribution of partial charges to shift between the two 3F conformers. This suggests that the two 3F conformers should have different Rydberg fingerprints and thus explains the congested nature of the spectrum of Figure 3.

To conclude this section, we summarize that the Rydberg fingerprint spectra are sensitive to the partial charge distributions within the molecular ion core. Even small changes in the molecular structure can lead to significant shifts of the charge center, which in turn causes large differences in the partial charge distributions about those charge centers. The electron is very sensitive to such changes, giving rise to Rydberg fingerprints that are very sensitive to the molecular geometry.

Global Structure Sensitivity. Having discussed the sensitivity of Rydberg fingerprint spectroscopy to intricate structural details, we now address the sensitivity of the technique to the global structure of larger molecules. The important point here is that the electronic wave functions of Rydberg orbitals are delocalized over a large volume. For hydrogen atoms, the mean radius as a function of the principal quantum number n and the angular momentum quantum number l is given by[17]

$$\langle r \rangle_{nl} = n^2 a_0 \left\{ 1 + \frac{1}{2}\left(1 - \frac{l(l+1)}{n^2} \right) \right\}$$

For example, a 3p Rydberg orbit has a mean diameter of 1.3 nm, and a 5s state has a diameter of 4 nm. Although for molecular systems the mean radius depends, in addition, on the quantum defect and thus the structure of the molecule, the equation illustrates that for the range of quantum numbers of interest to our work the radii of Rydberg states are large compared to the dimensions of typical molecules. One is therefore led to surmise that the Rydberg fingerprint spectra should depend on the overall global structure of a molecule.

To test the validity of this conjecture, we recorded the Rydberg fingerprint spectra of a series of aliphatic diamines consisting of *N*,*N*,*N*′,*N*′-tetramethyl-methane-diamine (TMMDA), *N*,*N*,*N*′,*N*′-tetramethyl 1,2-ethanediamine (TMEDA), and *N*,*N*,*N*′,*N*′-tetramethyl 1,3-propanediamine (TMPDA). For these molecules, the sizes of even the $n = 3$ wave functions exceed the dimensions of the molecule. As a result, the wave functions of these Rydberg states should encompass the entire molecule. The Rydberg fingerprint spectra, obtained according to the scheme of Figure 2a, are shown in Figure 5. The three spectra were obtained using identical excitation conditions: two photons of wavelength 418 nm excite the molecule to the Rydberg states, and a third photon ionizes the molecule. Given the reported ionization potentials (IP) in the range of 7.59−7.74 eV,[18,19] the two-photon energy of 5.92 eV can access Rydberg states only up to $n = 3$.

All three Rydberg fingerprint spectra of Figure 5 show two dominant spectral features: a large peak at a binding energy of about 2.3 eV and a smaller one at about 2.8 eV. All of those peaks can be associated with $n = 3$ states, with quantum defects as indicated in the Figure. The most important observation is that the three molecules have Rydberg states with similar but distinctly different quantum defects. All molecules feature a peak with a quantum defect of about 0.8, which is likely due to the

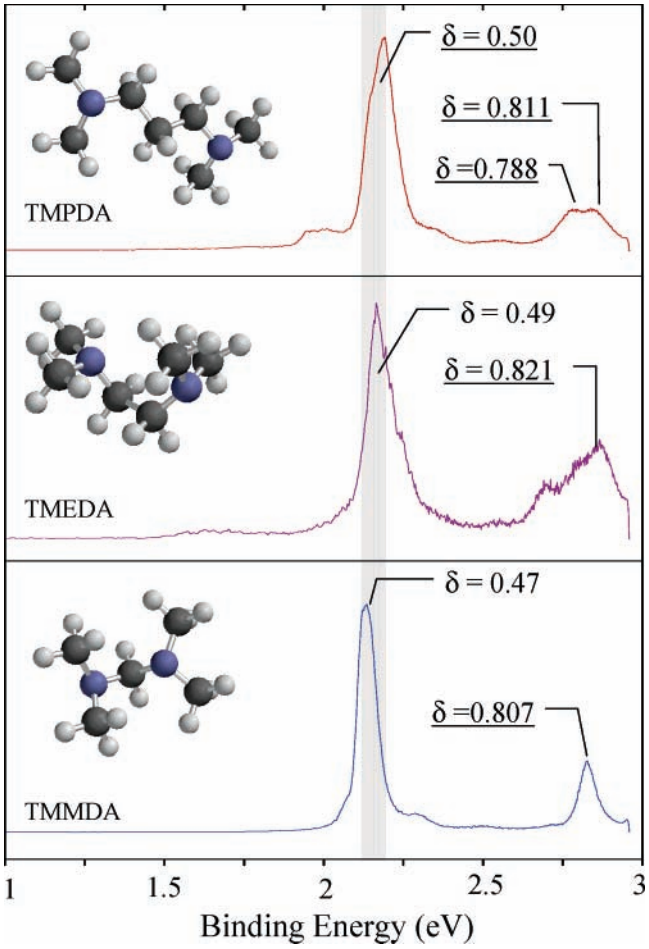

Figure 5. Rydberg fingerprint spectra of *N*,*N*,*N*′,*N*′-tetramethyl 1,3-propanediamine (top), *N*,*N*,*N*′,*N*′-tetramethyl-1,2-ethanediamine (middle), and *N*,*N*,*N*′,*N*′- tetramethyl-methane-diamine (bottom) obtained with laser pulses at 418 nm.

3s level. The peaks with quantum defects of about 0.5 probably arise from 3p orbits.

The ionization energies of the diamines under consideration here are near 7.6 eV, a value that is typical for tertiary amines with localized charges. We have separately measured the Rydberg fingerprint spectrum of tetrakis(dimethylamino)ethylene (TDMAE), a molecule where the charge of the cation is delocalized over the molecular frame. We found that the quantum defect of the dominant Rydberg series is 0.40 and that the ionization energy of TDMAE is about 5.4 eV, in agreement with the work of Soep et al.[20] Because two photons bring TDMAE above its ionization energy, many Rydberg levels are energetically accessible, giving rise to an extended series of peaks in the Rydberg fingerprint spectrum. Thus, the overall Rydberg fingerprint, the values of the quantum defects, and the ionization energies all suggest that the positive charges in our selection of diamines are localized on a single nitrogen atom.

The Rydberg fingerprint spectra of the diamines can be discussed within the framework developed for the fluorophenols. The Rydberg energies are primarily determined by the dominant Coulomb potential of the positive charge that is positioned at one of the amine atoms. Because in all molecules the nitrogen atom is surrounded by two methyl groups on one side and a CH_2 moiety on the other side, the similarity of the spectra is reasonable; the quantum defects of 0.48 ± 0.02 and 0.81 ± 0.01 are the fingerprints of the tertiary dimethylamines. Even so, the quantum defects of the diamines are not identical. With the positive charges pinned to one end of the molecule, the differences between the diamines at the far end of the molecules apparently affect the quantum defects. In the picture of the expansion of the electrostatic potential between the positive ion core and the electron, there are differences in the higher-order terms due to the varying lengths of the carbon chains. The addition of CH_2 groups alters the dipole and quadrupole moments, which induces changes in the potential energy and thus the energy of the Rydberg levels. In the description of the quantum defects as arising from phase shifts (Figure 1), the variation in the number of carbon atoms and the resulting displacement of the rest of the molecule gives rise to different phase shifts, which then cause different energies of the Rydberg states. Either way, it is easily seen that the change in the molecular structure, at parts of the molecule far removed from the charge center, gives rise to characteristic changes in the Rydberg spectra. We conclude that the Rydberg fingerprint spectra are sensitive to the global structure of the molecule.

Although the changes in the quantum defect values are the most important observation relating to the diamines, it is interesting to consider more subtle differences as well. The spectrum of TMMDA features two peaks that are sharp within the spectral resolution of the femtosecond laser spectrometer. The spectra of TMEDA and TMPDA, however, reveal slightly broadened peaks and possibly some structure underlying the smaller peak near 2.8 eV. Several reasons can be cited for the broadened spectra. First, it is possible that the larger amines are present in the molecular beam in several conformers. We have previously observed the Rydberg spectra of cyclic and open isomers of the C_6H_8 system and found that the open hexatrienes can exist in many conformeric forms.[4] As a result, the Rydberg fingerprints of those molecules are largely washed out. The diamines subject to the present discussion have more rigid structures, presumably on account of interactions involving the amine groups. Even so, it is possible that conformeric forms exist, for example, by inverting along the umbrella motion of an amine. It is reasonable to suggest that the larger molecules may have more conformeric forms at similar energy. The presence of several isomeric forms in the beam can give rise to broadened Rydberg fingerprint spectra. We note that the observed broadening supports the thesis of structure sensitivity of Rydberg states.

Summary, Perspectives, and Outlook

This article presents Rydberg fingerprint spectroscopy as an interesting new method to characterize molecular structures. Although at the present time it is difficult to obtain quantitative molecular structures by inversion of Rydberg spectra, the fingerprint nature of the spectra allows for comparison between similar compounds and suggests the creation of libraries. From the experiments described here, we derive an understanding of the intriguing ways in which Rydberg states probe molecular structures: as the loosely bound electron passes the ion core, it experiences a phase shift that is manifest in the level's energy. Conceptually, the phase shift is analogous to the phase shift that a free electron experiences when diffracting off a molecule. In that respect, one can understand Rydberg fingerprint spectroscopy as electron diffraction with bound electrons. Similarly, the Rydberg fingerprint technique is related to the scattering of electrons driven by the ac electric fields of intense laser pulses.[21,22]

Rydberg states probe molecular structures in a unique way. We have shown that the fingerprints are sensitive toward the charge distributions within aromatic molecules. Because the charge distributions can change even with the rotation of a single

hydrogen atom about a C−O bond axis, the Rydberg fingerprints are exquisitely sensitive toward the conformeric forms of such systems. However, the large size of Rydberg wave functions makes the fingerprints sensitive toward the global features of molecular structures. This aspect of structure characterization sets Rydberg fingerprints apart from other structural methods, all of which have sensitivities that are heavily tilted toward short-range structures. Although in those methods, which includes X-ray diffraction and NMR spectroscopy, the large-scale structure can be assembled from many short-range distances, Rydberg fingerprints offer the opportunity to characterize global molecular shapes directly. This feature may make the technique particularly important for the characterization of structures in nanoscience and in biological systems.

Several additional features of Rydberg fingerprint spectroscopy are of note. In particular, we point out that Rydberg fingerprints are almost completely insensitive to the temperature of the sample, save for the delocalization of the structure on account of large-amplitude motions. This property, which is unique for a spectroscopic technique, arises from the fact that the potential energy surfaces of Rydberg states are almost identical to those of the corresponding ion. Therefore, the ionization transitions are associated with $\Delta v = 0$ propensity rules and feature transition energies that are largely independent of the vibrational state. Evidence for this suggestion comes directly from our spectra: the three-photon excitation mechanism inserts about 1.1 to 2.3 eV of energy into vibrational coordinates in the fluorophenol systems. As a result, these molecules have, while in their respective Rydberg states, an amount of vibrational energy that exceeds the thermal excitation at ordinary temperatures. Even so, the spectral lines are sharp within the resolution of our instrument. In this context, it is interesting that the number of Rydberg states in a given energy range is not determined by the complexity of the molecule but instead is given by the quantum mechanics of the angular momentum states associated with specific principal quantum numbers.

In the presented data, we already have demonstrated that the Rydberg fingerprint spectra can be acquired in a multiplex fashion. Even so, the spectral resolution of the current instrument is marginal, and future improvements are desirable. Because the ionization is performed with ultrashort laser pulses, a combination of the Rydberg fingerprint method with time-resolved techniques lends itself to the observation of time-dependent structure changes. Work on both of these frontiers is forthcoming.

Limitations to the Rydberg fingerprint technique arise from the combination of spectral resolution and the number of molecular structures. As seen in the 3-fluorophenol system, our spectral resolution does not suffice to identify fingerprint spectra when several structures are present. Clearly, improved spectral resolution will help to overcome this limitation. A fundamental limitation arises, however, from the requirement that Rydberg states must exist. Thus, in its present form, the method is not applicable to negative ions.

Finally, we point out that the observation of Rydberg fingerprints can be made an integral part of the ionization process, which points toward the coupling of Rydberg fingerprint spectroscopy with mass spectrometry. The combination of laser photoionization with mass spectrometry is already well established,[23] although at present there are few incentives to use the technology, save for specific niche applications. Traditionally, photoionization for the purpose of mass spectrometry has been performed with nanosecond laser pulses and leads to significant fragmentation. In contrast, photoionization with ultrashort laser pulses is a soft ionization technique (i.e., it leads to very little fragmentation[24]). Because the Rydberg fingerprint technique works well with ultrashort laser pulses, this raises the intriguing possibility of designing an instrument that provides the parent mass as one output dimension and a shape-sensitive spectral fingerprint as a second dimension. The construction of such an instrument is underway. Given the global structure sensitivity, combined Rydberg fingerprint−mass spectrometry promises to become extremely interesting for large molecular systems.

Acknowledgment. We benefited immensely from discussions with Professor R. M. Stratt about the expansion of the electron−ion core interactions in a multipole series and from Professor M. B. Zimmt's guidance with the calculation of charge distributions in molecular ions. Gabriela Schlau-Cohen assisted with the acquisition of the data. Our research is supported by the Chemical Sciences, Geosciences and Biosciences Division, Office of Basic Energy Sciences, Department of Energy, grant number DE-FG02-03ER15452.

References and Notes

(1) Gallagher, T. F. *Rydberg Atoms*; Cambridge University Press: Cambridge, U.K., 1984.

(2) Freund, R. S. High-Rydberg Molecules. In *Rydberg States of Atoms and Molecules*; Stebbings, R. F., Dunning, F. B., Eds.; Cambridge University Press: Cambridge, U.K., 1983; pp 355−391.

(3) Rabalais, J. W. *Principles of Ultraviolet Photoelectron Spectroscopy*; John Wiley and Sons: New York, 1977.

(4) Kuthirummal, N.; Weber, P. M. *Chem. Phys. Lett.* **2003**, *378*, 647.

(5) Schick, C. P.; Weber, P. M. *J. Phys. Chem. A* **2001**, *105*, 3725.

(6) Schick, C. P.; Weber, P. M. *J. Phys. Chem. A* **2001**, *105*, 3735.

(7) Schick, C. P.; Carpenter, S. D.; Weber, P. M. *J. Phys. Chem. A* **1999**, *103*, 10470.

(8) Cheng, W.; Evans, C. V.; Kuthirummal, N.; Weber, P. M. *Chem. Phys. Lett*. **2001**, *349*, 405.

(9) Hennig, H.; Breidbach, J.; Cederbaum, L. S. *J. Phys. Chem. A* **2005**, *109*, 409.

(10) Cheng, W.; Kuthirummal, N.; Gosselin, J. L.; Sølling, T. I.; Weinkauf, R.; Weber, P. M. *J. Phys. Chem. A* **2005**, *109*, 1920.

(11) Kim, B.; Thantu, N.; Weber, P. M. *J. Chem. Phys.* **1992**, *97*, 5384.

(12) Maier, J. P.; Marthaler, O.; Mohraz, M. *J. Electron Spectrosc. Relat. Phenom*. **1980**, *19*, 11.

(13) Oikawa, A.; Abe, H.; Mikami, N.; Ito, M. *Chem. Phys. Lett.* **1985**, *116*, 50.

(14) Yosida, k.; Suzuki, S.; Sakai, M; Fujii, M.; Dessent, C. E. H.; Müller-Dethlefs, K. *Phys. Chem. Chem. Phys.* **2002**, *4*, 2534.

(15) Cohen-Tannoudji, C.; Diu, B.; Laloë, F. *Quantum Mechanics*; John Wiley and Sons: New York, 1977; Vol. 2, Chapter E_x.

(16) Jackson, J. D. *Classical Electrodynamics*, 2nd ed.; John Wiley & Sons: New York, 1975; Chapter 4.

(17) Atkins, P. W.; Friedman, R. S. *Molecular Quantum Mechanics*, 3rd ed.; Oxford University Press: Oxford, U.K., 1997; p 94.

(18) Loguinov, T.; Takhistov, V. V.; Vatlina, L. P. *Org. Mass Spectrom* **1981**, *16*, 239.

(19) Livant, P.; Roberts, K. A.; Eggers, M. D.; Worley, S. D. *Tetrahedron* **1981**, *37*, 1853.

(20) Soep, B.; Mestdagh, J. M.; Sorgues, S.; Visticot, J. P. *Eur. Phys. J. D* **2001**, *14*, 191−203.

(21) Spanner, M.; Smirnova, O.; Corkum, P. B.; Ivanov, M. Y. *J. Phys. B: At. Mol. Opt. Phys.* **2004**, *37*, L243.

(22) Itatani, J.; Levesque, J.; Zeidler, D.; Niikura, H.; Pe'pin, H.; Kieffer, J. C.; Corkum, P. B.; Villeneuve, D. M. *Nature* **2004**, *432*, 867.

(23) Lubmann, D. M. Lasers and Mass Spectrometry. *Optical Sciences*; Oxford Series; Lapp, M., Stark, H., Eds.; Oxford University Press: Oxford, U.K., 1990.

(24) Carpenter, S. D.; Schick, C. P.; Weber, P. M. *Rev. Sci. Instrum.* **1999**, *70*, 2262.